Experimental Gerontology 126 (2019) 110691

Contents lists available at ScienceDirect

Experimental Gerontology

journal homepage: www.elsevier.com/locate/expgero

Mitochondrial metabolic reprograming via BRAF inhibition ameliorates senescence

Jae Won Kim[a,1], Myeong Uk Kuk[a,1], Hyon E. Choy[b], Sang Chul Park[c,d,*], Joon Tae Park[a,**]

[a] Division of Life Sciences, College of Life Sciences and Bioengineering, Incheon National University, Incheon, Republic of Korea
[b] Department of Molecular Medicine, Chonnam National University Medical School, Gwangju, Republic of Korea
[c] Well Aging Research Center, Daegu Gyeongbuk Institute of Science and Technology, Daegu, Republic of Korea
[d] The Future Life & Society Research Center, Chonnam National University, Gwangju, Republic of Korea

ARTICLE INFO

Keywords:
BRAF
SB590885
Senescence
Mitochondrial function
Metabolic reprogramming

ABSTRACT

Senescence is defined as irreversible cell cycle arrest and constitutes a major driving force in diseases related to aging or premature aging. Recent studies indicate that activation of the serine/threonine protein kinase B-raf (BRAF) plays important roles in oncogene-induced senescence. However, it remains elusive whether BRAF inhibition might be effective for abrogating senescence. In this study, we assessed several BRAF inhibitors to identify compounds that ameliorate senescence and revealed SB590885 as an effective agent. Senescence-ameliorating effect upon BRAF inhibition was evident from the observation that SB590885 treatment increased cellular proliferation but diminished senescent phenotypes. Moreover, BRAF inhibition induced the mitochondrial functional recovery along with the metabolic reprogramming, which comprises two salient features that are altered in senescent cells. Furthermore, mitochondrial metabolic reprogramming via BRAF inhibition was a prerequisite for senescence amelioration. Taken together, our data revealed a novel mechanism in which senescence amelioration is mediated by mitochondrial metabolic reprogramming upon BRAF inhibition.

1. Introduction

Senescence is defined as a state in which normal somatic cells lose their replicative capacity (Bolden and Lowe, 2015). Somatic cells proliferate for a finite number of divisions and no longer divide as they become senescent (Bolden and Lowe, 2015). In addition to cell cycle arrest, senescent cells develop a distinctive morphology including an increase in number and size of mitochondria (Dimri et al., 1995). This increase is largely attributed to the accumulation of dysfunctional mitochondria, which produce more reactive oxygen species (ROS) (Hwang et al., 2009). As the main sources of ROS generation, dysfunctional mitochondria are the major targets of ROS-induced damage, consequently leading to the damage in the electron transport complex (ETC) (Houtkooper et al., 2011; James et al., 2015). The altered ETC leads to a decrease in oxidative phosphorylation (OXPHOS) accompanied by reduction in ATP generation. Thus, senescent fibroblasts show higher dependency on glycolysis than OXPHOS for an energy source (Lin et al., 2001). Alterations in energy metabolism are linked to the aging process and aging-associated diseases (Barzilai et al., 2012). However, the underlying mechanism to reverse the altered mitochondrial metabolism remains elusive. Thus, there is a need for mechanism-based strategies to modulate mitochondrial metabolic reprogramming.

Oncogene-induced senescence (OIS) is a complex program triggered by the abnormal activation of oncogenic signals (Liu et al., 2018). OIS is a robust and persistent antiproliferative response caused by activation of an oncogene (Liu et al., 2018). OIS was first observed following expression of an oncogenic RAS in normal human fibroblasts (Serrano et al., 1997). Paradoxically, the RAS-RAF-MEK-ERK signaling cascade triggers cell cycle arrest through activation of the RB and p53 pathways (Kilbey et al., 2008). This process is similar to replicative senescence, a phenomenon observed in aged cultures of primary human fibroblasts, which is generally due to the loss of proliferative capacity (Patil et al., 2005). RAF signaling serves as an immediate downstream effector of RAS and activates MEK, which in turn activates ERK (Cheng et al., 2018). As a member of the RAF kinase family, BRAF functions as a serine/threonine protein kinase (Sithanandam et al., 1990). BRAF

* Correspondence to: S.C. Park, Well Aging Research Center, DGIST, Daegu, Republic of Korea
** Correspondence to: J.T. Park, Division of Life Sciences, College of Life Sciences and Bioengineering, Incheon National, 119 Academy-ro, Yeonsu-gu, Incheon 22012, Republic of Korea
E-mail addresses: scpark@snu.ac.kr (S.C. Park), joontae.park@inu.ac.kr (J.T. Park).
[1] These authors contributed equally to this work.

https://doi.org/10.1016/j.exger.2019.110691
Received 25 April 2019; Received in revised form 8 August 2019; Accepted 12 August 2019
Available online 14 August 2019
0531-5565/ © 2019 Elsevier Inc. All rights reserved.

activation is observed in human cancers and is sufficient to transform established lines toward neoplastic growth (Ascierto et al., 2012). However, in cultures of normal fibroblasts, BRAF exerts paradoxical effects including cell cycle arrest and apoptosis (Zhu et al., 1998). Specifically, BRAF activation in normal fibroblasts elicited senescence accompanied by the increased expression of p53, p21, and p16 (Zhu et al., 1998). Thus, the strategy for applying BRAF inhibition in normal fibroblasts might be worth testing for senescence amelioration.

In the present study, we aimed to evaluate whether BRAF inhibition might constitute an effective strategy to ameliorate senescence. To address this possibility, we screened several BRAF inhibitors and identified SB590885 as an effective agent. Here, we demonstrated a novel mechanism in which senescence amelioration was controlled by BRAF inhibition-induced mitochondrial metabolic reprogramming.

2. Materials and methods

2.1. Drug screening

Senescent fibroblasts were grown in 96-well plates at a density of 2000 cells per well. Components of the BRAF inhibitor library (Selleck Chem) were diluted to a final concentration of 0.5 μM and added to the wells every 4 days. The BRAF inhibitor library included SB590885 (S2220), vemurafenib (S1267), TAK-632 (S729), CEP-32496 (S8015), GDC-0879 (S1104), PLX-4720 (S1152), sorafenib tosylate (S1040), sorafenib (S7397), GW5074 (S2872), ZM 336372 (S2720), dabrafenib (S2807), AZ 628 (S2746), RAF265 (S2161), and NVP-BHG712 (S2202). BRAF inhibitor library and dimethylsulfoxide (DMSO) (D8148; Sigma, St. Louis, MO, USA) were diluted to a final concentration of 0.5 μM and 1.4 mM in the culture medium, respectively. At 21 days after drug treatment, cells were washed twice with phosphate-buffered saline (PBS) and lysed in 50 μl of 0.2% sodium dodecyl sulfate. The plates were incubated at 37 °C for 2 h. SYBR Green I (150 μl) nucleic acid gel stain (1:1000 in DW; S-7567; Molecular Probes, Eugene, OR, USA) was added to the wells. Cell number was determined by measuring fluorescence intensity using a fluorescence microplate reader (Infinite 200 PRO; Tecan Life Sciences, Männedorf, Switzerland). The mean and standard deviation from six replicates were determined for each experimental group.

2.2. Cell culture

Human diploid fibroblasts (PCS-201-010; American Type Culture Collection, Manassas, VA, USA) were used in this study. Cells were cultured in Dulbecco's modified Eagle's medium containing 25 mM glucose supplemented with 10% fetal bovine serum (SH30919.03; Hyclone; Waltham, MA, USA) along with 100 U/ml penicillin and 100 μg/ml streptomycin (SV30079.01; Hyclone). Confluent cells were split 1:4 and 1:2 during early and late passages, respectively. The number of population doublings (n) was calculated using the equation: $n = \log_2 F / I$, where F and I are the number of cells at the end and number seeded at the beginning of one passage, respectively. When the population doubling time of the cells was over 14 days and < 2 days, the cells were considered senescent and young, respectively. Cells were tested for mycoplasma contamination every other week by using the, MYCOALERT MYCOPLASMA DETECTION kit (LT07-318; Lonza, Basel, Switzerland). To perform the functional assay, cells were treated with DMSO or SB590885 for 21 days.

2.3. Senescence-associated β-galactosidase (SA-β-gal) staining

SA-β-gal assays were carried out via either a quantitative chemiluminescence assay or X-Gal cytochemical staining. The quantitative chemiluminescence assay was performed using a modified protocol with the Galacto-light System (Bassaneze et al. 2013). Briefly, cells were plated in 6 well plates. After 2 days, cells were washed twice with PBS and lysed in 50 μl of cell culture lysis buffer. Next, 5 μl lysate was incubated with galacton substrate in 200 μl of reaction buffer (20 μM $MgCl_2$, 100 mM sodium phosphate, pH 6.0) for 40 min at room temperature, and then 300 μl of Emerald Luminescence Amplifier was added immediately before measurement with a luminometer. The values were normalized by total protein amount in the sample. Bradford assays were used to quantify protein. X-Gal cytochemical staining for

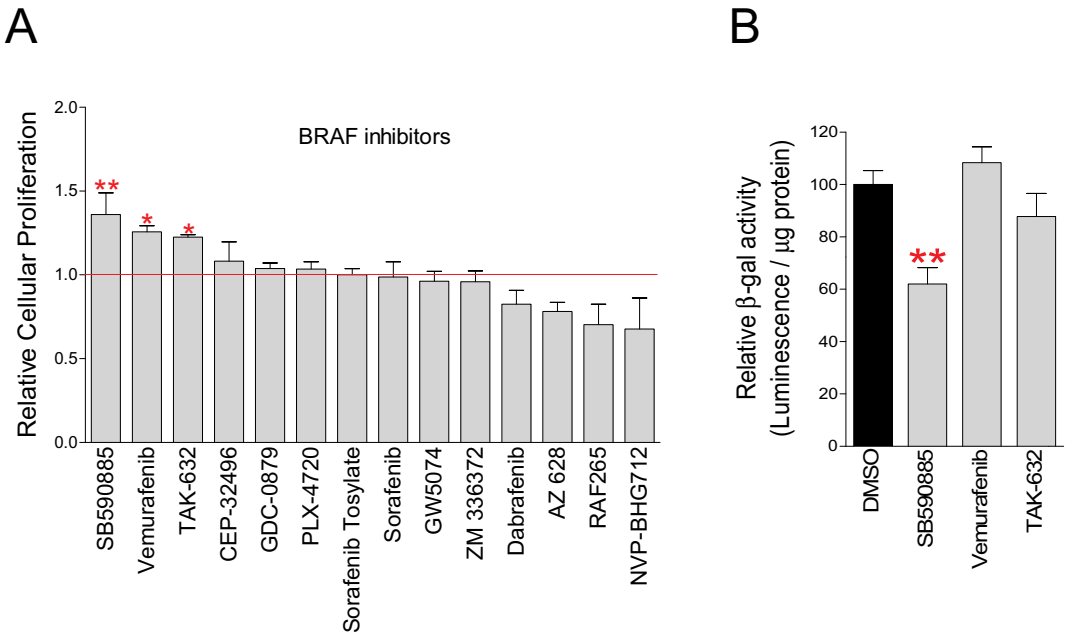

Fig. 1. Chemical screening for agents that alleviate senescence among BRAF inhibitors. (A) DNA content-based method to measure cell number (*$P < 0.05$, **$P < 0.01$, Student's *t*-test). Means ± S.D., N = 3. (B) SA-β-gal activity was measured quantitatively using galacton as the substrate (**$P < 0.01$, Student's t-test). Means ± S.D., N = 3.

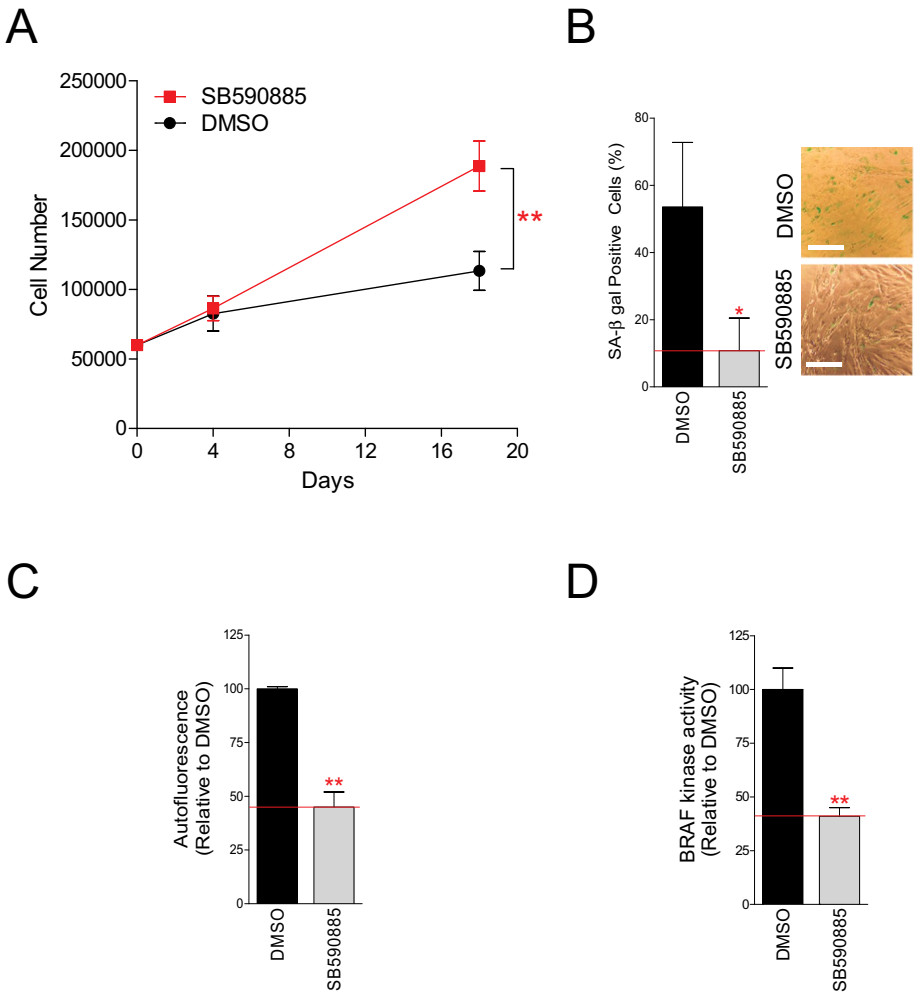

Fig. 2. BRAF as a potential target for ameliorating senescence. (A) Confirmation of the proliferation-inducing effect observed in screening by measuring cellular proliferation at the multiple time points (**$P < 0.01$, two-way ANOVA followed by Bonferroni's post test). Means ± S.D., N = 3. (B) Quantification of SA-β gal positive cells (*$P < 0.05$, Student's t-test; scale bar 20 μm). Means ± S.D., N = 3. (C) Effects of SB590885 treatment on lipofuscin accumulation (**$P < 0.01$, Student's t-test). Mean ± S.D., N = 3. (D) BRAF kinase assay to examine the specificity of SB590885 as a BRAF inhibitor (**$P < 0.01$, Student's t-test). Mean ± S.D., N = 3.

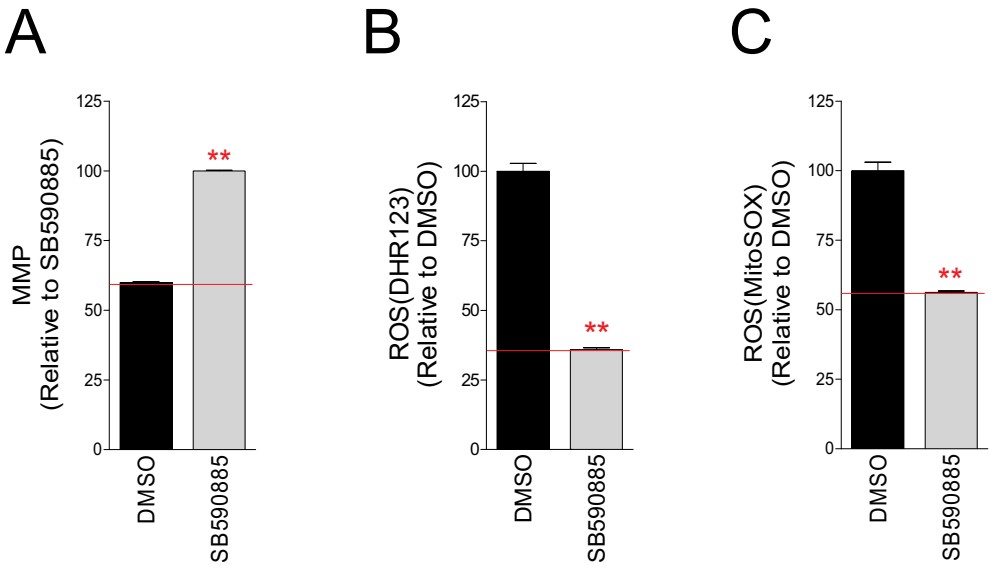

Fig. 3. Effect of BRAF inhibition on the mitochondrial function. (A) Flow cytometric analysis of MMP using JC-10 (**$P < 0.01$, Student's t-test). Means ± S.D., N = 3. (B and C) Flow cytometric analysis of mitochondrial ROS using DHR123 (B) and mitochondrial ROS using MitoSOX (C) (**$P < 0.01$, Student's t-test). Means ± S.D., N = 3.

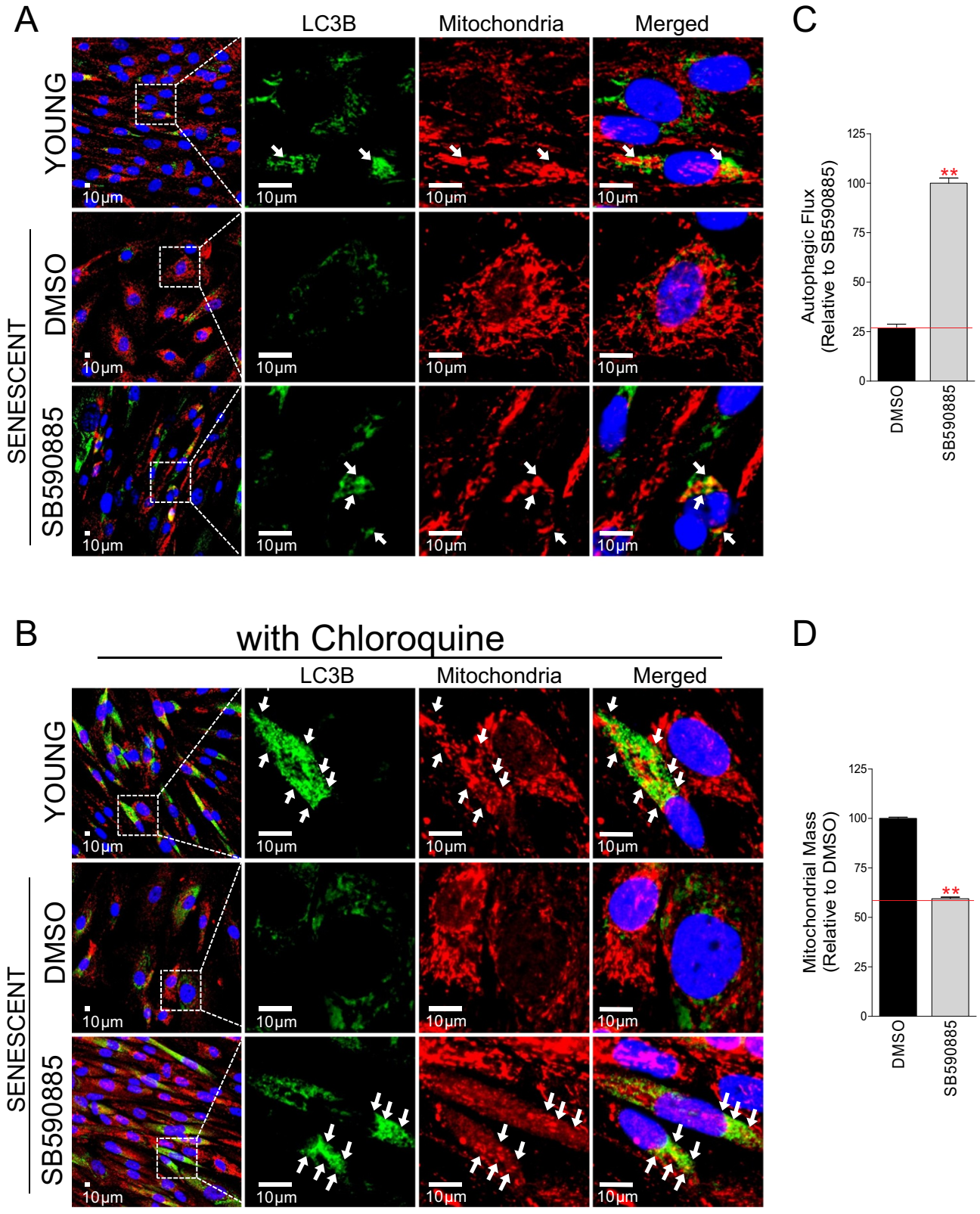

Fig. 4. Removal of dysfunctional mitochondria through the activation of mitophagy. (A) Immunostaining for LC3B (green) and mitochondria (red) (scale bar 10 μm). (B) Immunostaining for LC3B (green) and mitochondria (red) after CQ treatment (scale bar 10 μm). (C) Flow cytometric analysis of autophagic flux using Cyto-ID (**$P < 0.01$, Student's t-test). Means ± S.D., N = 3. (D) Flow cytometric analysis of mitochondrial mass using MitoTracker Green (**$P < 0.01$, Student's t-test). Means ± S.D., N = 3. (For interpretation of the references to color in this figure legend, the reader is referred to the web version of this article.)

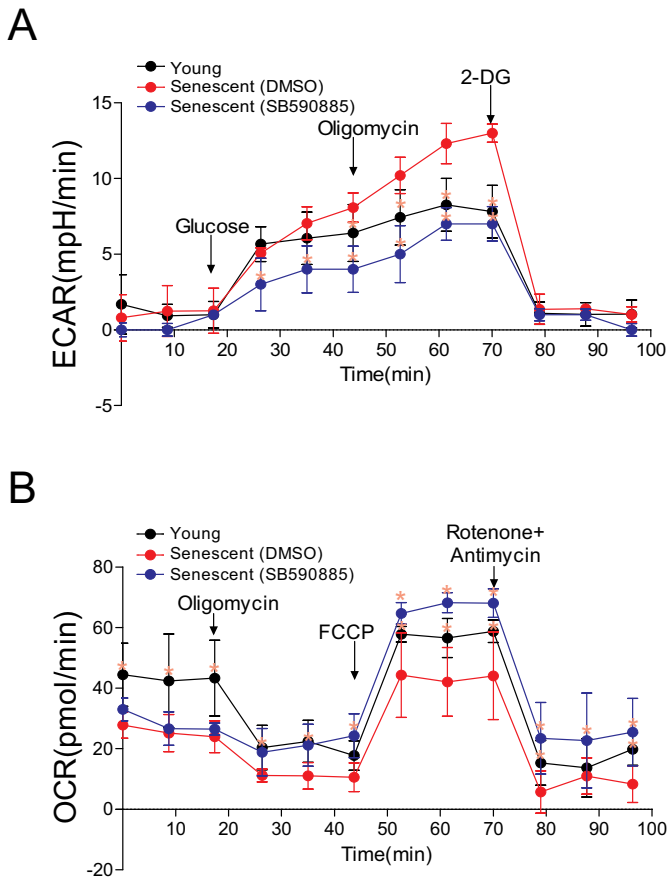

Fig. 5. BRAF regulates mitochondrial function by inducing metabolic reprogramming. (A) Measurement of ECAR (black line: young fibroblasts, blue line: SB590885-treated senescent fibroblasts, and red line: DMSO-treated senescent fibroblasts) (**$P < 0.01$, two-way ANOVA followed by Bonferroni's post test). Means ± S.D., N = 3. (B) Measurement of OCR (black line: young fibroblasts, blue line: SB590885-treated senescent fibroblasts, and red line: DMSO-treated senescent fibroblasts) (**$P < 0.01$, two-way ANOVA followed by Bonferroni's post test). Means ± S.D., N = 3. (For interpretation of the references to color in this figure legend, the reader is referred to the web version of this article.)

SA-β-gal was performed according to the manufacturer's protocols (9860; Cell Signaling Technology, Danvers, MA, USA).

2.4. BRAF kinase assay

Prior to the in vitro kinase assay, senescent fibroblasts were treated with 00.1 μM SB590885 or 0.28 mM DMSO for 14 days. Then, cells were lysed using 1 × kinase buffer with 10 mM DTT (43816; Sigma) for BRAF kinase assay. Protein concentration was determined by using Pierce™ BCA Protein Assay Kit (23227; Thermo Fischer Scientific, Waltham, MA, USA). In each kinase reaction, 1.2 μg of cell lysates was used and the kinase assay was performed according to the manufacturer's protocols (48688; BPS bioscience, San Diego, CA, USA).

2.5. Measurement of reactive oxygen species (ROS) and mitochondrial membrane potential (MMP)

For quantification of mitochondrial ROS, the cells were incubated in medium containing 30 μM DHR123 (D632; Life Technologies, Carlsbad, CA, USA) and 5 μM MitoSOX (M36008; Life Technologies) for 30 min at 37 °C. For quantification of mitochondrial mass, the cells were incubated in medium containing 50 nM MitoTracker deep red (M22426; Life Technologies) for 30 min at 37 °C. For measurement of MMP, the cells were incubated with 0.6 μg/ml JC-10 (ENZ-52305; Enzo Life Sciences, Farmingdale, NY, USA) for 30 min at 37 °C. After staining, cells were prepared for fluorescence-activated cell sorting analysis as previously described (Kang and Hwang, 2009). Results were analyzed using Cell Quest 3.2 software (Becton Dickinson, Bedford, MA, USA).

2.6. Flow cytometric analysis of cellular lipofuscin levels

Lipofuscins are mainly produced through the peroxidation of unsaturated fatty acids in complex with proteins. They are autofluorescent consequent to the Schiff base formed by the reaction between carbonyl and amino compounds (Marani et al., 2009). A highly utilized method for quantification of lipofuscin is based on the assessment of autofluorescence (Cho and Hwang, 2011; Jensen et al., 2016; Jung et al., 2010; Moore et al., 1995). Specifically, for quantitation of autofluorescence, cells were washed with PBS, trypsinized, collected in PBS, and analyzed by flow cytometry according to the settings for FITC (530/30 nm bandpass filters with excitation at 488 nm). Results were analyzed using Cell Quest 3.2 software (Becton Dickinson).

2.7. Immunofluorescence

For immunofluorescence, cells plated on Nunc Lab-Tek II Chamber Slide (154526; Thermo Fischer Scientific) were fixed with 4% paraformaldehyde in PBS for 15 min at room temperature and then permeabilized with 0.1% Triton X-100 in PBS for 15 min. Blocking was carried out with 10% FBS in PBS at room temperature for 1 h. Samples were incubated with primary antibodies diluted in 10% FBS in PBS overnight at 4 °C. After incubation with rabbit anti-LC3B antibody (2775; 1:200 dilution; Cell Signaling Technology) and mouse anti-mitochondria antibody (MS601; 1:1000 dilution; MitoSciences, Eugene, OR, USA), the cells were washed with ice-cold PBS three times and incubated with Alexa Fluor 488-conjugated anti-rabbit antibody (A-11008; 1:1000 dilution; Invitrogen, Carlsbad, CA, USA) and Alexa Fluor 594-conjugated anti-mouse antibody (A-21201; 1:1000 dilution; Invitrogen) for 1 h at RT. The nuclei were then stained with DAPI (R37606; Invitrogen) and samples were mounted using ProLong Gold Antifade reagent (P36934; Invitrogen). Images were captured using a Carl Zeiss Axio Imager Z1 microscope.

2.8. Measurement of autophagic flux

Autophagic flux was measured using a Cyto-ID as described previously (Guo et al., 2015), with minor modifications. Briefly, cells were incubated in medium containing 20 μM CQ. At 12 h after incubation, cells were further stained with Cyto-ID staining solution and prepared for FACS analysis. Autophagic flux was calculated using the following equation: ΔMFI (mean fluorescence intensity) Cyto-ID = MFI Cyto-ID (+CQ) − MFI Cyto-ID (−CQ).

2.9. Seahorse analysis

The XFe24 flux analyzer (Seahorse Bioscience, Billerica, MA, USA) was used according to the manufacturer protocol. Briefly, 5×10^4 cells were distributed into each well of an XFe24 cell-culture plate from the XF24 FluxPak (100850-001; Seahorse Bioscience) and then cultured in a 5% CO_2 incubator at a temperature of 37 °C for 16 h. Next, the medium was replaced by XF Assay medium (102365-100; Seahorse Bioscience), which lacked glucose, and the cells were then cultured for another 1 h in the same incubator. The extracellular acidification rate (ECAR; mpH/min) was measured using an XF Glycolysis Stress Test kit (102194-100; Seahorse Bioscience). The oxygen consumption rate (OCR; pmol/min) was measured using an XF Cell Mito Stress Test Kit (101706-100; Seahorse Bioscience).

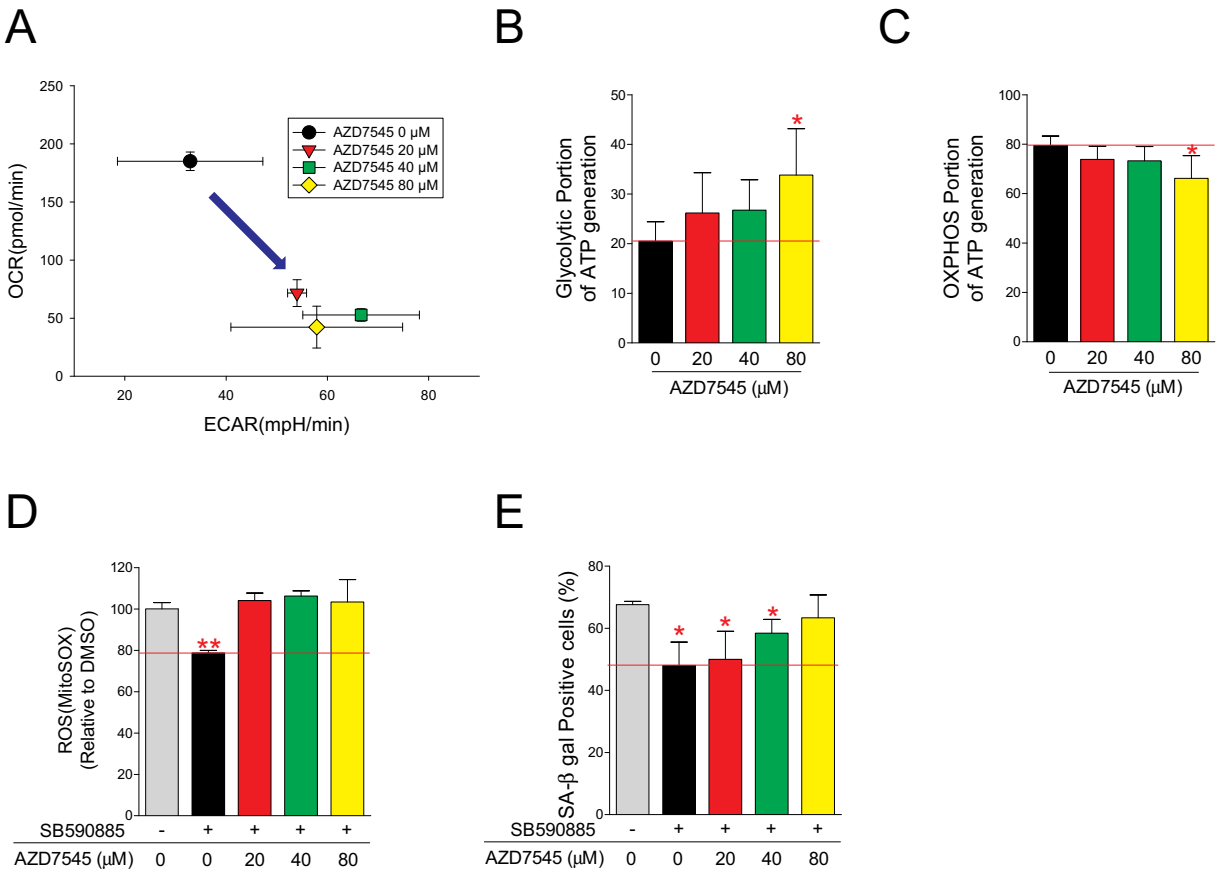

Fig. 6. Metabolic reprogramming by BRAF inhibition is a prerequisite for senescence amelioration. (A) Measurement of ECAR and OCR after AZD7545 treatment. Means ± S.D., N = 6. (B and C) Glycolytic and OXPHOS portion of ATP generation (*$P < 0.05$, one-way ANOVA with Bonferroni's multiple comparison test). Means ± S.D., N = 6. (D) Flow cytometric analysis of mitochondrial ROS using MitoSOX (**$P < 0.01$, Student's t-test). Means ± S.D., N = 3. (E) Quantification of SA-β gal positive cells (*$P < 0.05$, Student's t-test; scale bar 20 μm). Means ± S.D., N = 3.

2.10. Measurement of cellular ATP levels

Cells were incubated in medium with or without 20 μM oligomycin (O4876; Sigma) for 24 h and then lysed with lysis buffer. ATP content was measured using a ViaLight Plus Kit (LT07-221; Lonza) according to the manufacturer's instructions. DNA content was measured using AccuBlue broad range dsDNA quantitation kit (31007; Biotium, Fremont, CA, USA). For measurements of relative ATP content, the luminescence of each sample was normalized to the DNA content.

2.11. Statistical analyses

Statistical analyses were performed using a standard statistical software package (SigmaPlot 12.5; Systat Software, San Jose, CA, USA). The Student's *t*-test, two-way ANOVA followed by Bonferroni's post test, or one-way ANOVA with Bonferroni's multiple comparison test was used to determine whether differences were significant.

3. Results

3.1. Chemical screening for agents that alleviate senescence by BRAF inhibition

The present screening strategy comprised two different methods for measuring the capacity for alleviating senescence: 1) increasing cell numbers, and 2) reducing SA-β-gal activity. For the primary screen, a DNA content-based method was used to accurately measure the cell number (Silva et al., 2013). A library containing 14 BRAF inhibitors was added to senescent fibroblasts and the effect of each inhibitor on cell proliferation was determined on day 21 (Fig. 1A). Inhibitors leading to more than a 1.3-fold increase were considered potential hits. Three compounds (SB590885, vemurafenib, and TAK-632) were identified as candidate drugs (Fig. 1A). A second round of screening was performed to quantitatively measure SA-β-gal activity level using a chemiluminescence method (Bassaneze et al. 2013). Among the three drugs, SB590885 was found to reduce SA-β-gal activity to 62% of the DMSO control (Fig. 1B) and was selected as a candidate agent for ameliorating the senescence phenotype.

To confirm the proliferation-inducing effect observed in screening, cellular proliferation was measured at the multiple time points. SB590885 treatment increased cellular proliferation compared to that of the DMSO control (Fig. 2A). Furthermore, to confirm SA-β-gal activity reduction, SA-β-gal positive cells were counted. Upon SB590885 treatment, the percentage of SA-β-gal positive cells was significantly reduced (Fig. 2B). Senescence amelioration by SB590885 was further determined based on the accumulation of lipofuscin, a common feature of senescence (Brunk and Terman, 2002). The lipofuscin level was ascertained by measuring intracellular levels of autofluorescence (Tohma et al., 2011). The lipofuscin level was significantly decreased by SB590885 (Fig. 2C).

To evaluate the specificity of SB590885 as a BRAF inhibitor, BRAF kinase assay using BRAF substrate was performed. SB590885-treated cell lysates exhibited the significantly decreased BRAF kinase activity compared to DMSO-treated cell lysates, confirming that the addition of SB590885 to the cultured cells efficiently inhibits BRAF activity (Fig. 2D).

3.2. BRAF inhibition yields functional recovery of mitochondria

BRAF has been shown to function as a major regulator of mitochondrial function in melanoma cells (Haq et al., 2014). As mitochondrial functional recovery constitutes a prerequisite for senescence amelioration (Kang et al., 2017b), we evaluated the effect of BRAF inhibition on mitochondria functional status. Upon SB590885 treatment, MMP was recovered, suggestive of mitochondrial functional recovery (Fig. 3A). Dysfunctional mitochondria comprise the major source of excessive ROS production, which causes severe damage in intracellular molecules and cellular organelles (Hwang et al., 2009). We then measured ROS levels by using two different dyes: DHR123 for hydroxyl radicals and hydrogen peroxides, and MitoSox for superoxide anions. Upon SB590885 treatment, ROS levels were significantly reduced (Fig. 3B and C).

We then examined the effect of the BRAF inhibition on mitophagy. Colocalization between mitochondria and the autophagosome marker LC3B was observed in young but rarely in senescent fibroblasts (Fig. 4A; white arrows). Upon SB590885 treatment, colocalization between mitochondria and LC3B re-appeared (Fig. 4A; white arrows). To confirm that BRAF inhibition induced mitophagy, we co-treated cells with chloroquine (CQ), which inhibits autophagic flux through the disruption of lysosomal pH (Shintani and Klionsky, 2004). As expected, CQ treatment increased autophagosome accumulation (LC3B, green) along with their colocalization with mitochondria in SB590885-treated senescent fibroblasts but not in DMSO controls (Fig. 4B; white arrows). Concomitant with the increased colocalization, autophagic flux was increased and mitochondrial mass was decreased, suggesting that mitophagy activation was achieved via BRAF inhibition (Fig. 4C and D).

3.3. BRAF inhibition induces metabolic reprogramming

To further assess mitochondrial functional recovery, mitochondrial metabolism was examined. The extracellular acidification rate (ECAR; mpH/min) was measured as an indicator of glycolysis (Brand and Nicholls, 2011). The compounds (glucose, oligomycin, and 2-deoxy-D-glucose (2-DG)) are serially injected to measure the glycolysis level including glycolysis, glycolytic capacity, and glycolytic reserve, respectively (Brand and Nicholls, 2011). The observed ECAR rate of senescent fibroblasts was higher than that of young fibroblasts, implying that senescent fibroblasts consumed more oxygen and showed more dependency on glycolysis to meet energy demands (Fig. 5A; black line vs. red line). However, SB590885 treatment recovered ECAR to a level similar to that of young fibroblasts (Fig. 5A; blue line vs. red line).

As we observed that BRAF regulates glycolysis levels, we hypothesized that BRAF also regulates OXPHOS efficiency. To confirm this, the oxygen consumption rate (OCR; pmol/min) was measured as an indicator of mitochondrial respiration (Brand and Nicholls, 2011). The compounds (oligomycin, carbonyl cyanide-*p*-trifluoromethoxyphenylhydrazone (FCCP), and a mixture of rotenone and antimycin A) were serially injected to measure the mitochondrial respiration rate including ATP production, maximal respiration, and nonmitochondrial respiration, respectively. Senescent fibroblasts demonstrated lower OCR than young fibroblasts, implying that senescent fibroblasts exhibited a defective mitochondrial respiration (Fig. 5B; black vs. red line). However, SB590885 treatment recovered OCR to a level similar to that of young fibroblasts (Fig. 5B; black vs. red line).

Taken together, BRAF inhibition induced mitochondria metabolic reprogramming from glycolysis to OXPHOS.

3.4. Metabolic reprogramming by BRAF inhibition is a prerequisite for senescence amelioration

We examined whether SB590885-induced metabolic reprogramming is a prerequisite for senescence amelioration. To inhibit OXPHOS, we used AZD7545, an inhibitor of pyruvate dehydrogenase kinase 2 (PDK2), which blocks the acetyl-CoA generation (Mayers et al., 2003). AZD7545 treatment shifted mitochondrial metabolism from OXPHOS to glycolysis (Fig. 6A). Moreover, the glycolytic part of ATP generation was increased but the OXPHOS part was reduced upon AZD7545, confirming its role as an inhibitor of OXPHOS (Fig. 6B and C). We then co-treated cells with SB590885 and AZD7545. AZD7545 treatment prevented the SB590885-induced recovery of mitochondrial function, through increasing ROS levels (Fig. 6D). Furthermore, AZD7545 treatment blocked the SB590885-induced diminishment of the senescent phenotypes including SA-β-gal activity (Fig. 6E). These data suggest that mitochondrial metabolic reprogramming by BRAF inhibition is a prerequisite for senescence amelioration.

4. Discussion

The maintenance of mitochondrial metabolism is closely linked to the control of senescence. Deterioration in mitochondrial metabolism is age dependent, as shown by cells acquired from aged animals exhibiting more dependency on glycolysis as an energy source (James et al., 2015). Moreover, alteration of mitochondrial metabolism in senescent cells may contribute to premature organ decline (Din et al., 2014); however, the means by which to delay or prevent this alteration are poorly explored. In the present study, we identified that BRAF mediates a novel mechanism to regulate senescence by the control of mitochondrial metabolic reprogramming. Upon BRAF inhibition, metabolic reprogramming was induced through shifting an energy source from glycolysis to OXPHOS. Furthermore, the adjusted mitochondrial metabolism by a PDK2 inhibitor, AZD7545, prevented the BRAF inhibitor-induced restoration of senescent markers, implicating that mitochondrial metabolic reprogramming by BRAF inhibition constitutes a prerequisite for senescence alleviation. To our knowledge, our study provides the first demonstration that BRAF inhibition induced mitochondrial metabolic reprogramming, rendering the targeting of mitochondrial metabolism as a potentially advantageous therapeutic strategy.

Mitochondria have long been studied in the context of their classic functions, as energy factories. They are now also recognized as a broad signaling platform that regulates many of the key elements of cell and tissue physiology (Ohya et al., 1991). These organelles thus comprise much more than simple industrial units, with mounting evidence supporting their crucial roles in the control of senescence (Kang et al., 2017a; Kang et al., 2017b; Kuk et al., 2019; Park et al., 2018). We have reported that inhibition of several protein kinase activities reversed back to juvenile status of mitochondrial function, coupled with senescence amelioration (Kang et al., 2017a; Kang et al., 2017b; Kuk et al., 2019; Park et al., 2018). For example, inhibition of rho-associated protein kinase (ROCK) restores mitochondrial respiration by dephosphorylating Rac1b, concomitant with ROS reduction (Kang et al., 2017a; Park et al., 2018). This reduction is accompanied by the increased efficiency of OXPHOS and the diminished dependency on glycolysis as an energy source (Kang et al., 2017a; Park et al., 2018). In addition, inhibition of ATM serine/threonine kinase induced lysosomal re-acidification, which in turn accelerated the removal of dysfunctional mitochondria, coupled with mitochondrial functional recovery and metabolic reprogramming (Kang et al., 2017b). In accordance with these findings, this study also found that inhibition of BRAF kinase activity induced mitochondrial functional recovery with senescence alleviation. Given the findings that the simple modulation of protein kinase activities can ameliorate mitochondrial function with senescence alleviation, the investigation of the underlying ROCK, ATM and BRAF signal pathway may provide important evidence toward finding the common therapeutic target for a novel aging control mechanism.

BRAF has a broad range of putative substrates that are involved in regulating the MAP kinase/ERK signaling pathway, which affects cell division and differentiation (Hussain et al., 2015). To maintain cellular homeostasis, BRAF orchestrates the activities of its substrates in

response to various stresses (Hussain et al., 2015). Therefore, to effect therapeutic targeting of BRAF, its activity should be adjusted using sophisticated strategies. The need for this careful approach may be inferred by evidence that BRAF inhibition causes side effects including the development of squamous cell carcinomas and recurrent tumors (Pérez-Lorenzo and Zheng, 2012). Accordingly, although we demonstrated that finely tuned BRAF activity via a chemical approach was beneficial in ameliorating senescence, the potential risk of BRAF inhibition remains and the therapeutic application of BRAF inhibition should be approached with caution.

In summary, our findings suggested a novel mechanism by which BRAF inhibition induces the rescue from cellular senescence. In particular, BRAF inhibition induced the restorative effect via the mitochondrial metabolic reprogramming, which functioned as a prerequisite for senescence amelioration. Taken together, our results provide evidence that the proper control of BRAF activity may represent a therapeutic target for alleviating senescence and might be clinically applicable to control age-related diseases.

Acknowledgments

This research was supported by Basic Science Research Program through the National Research Foundation of Korea (NRF) funded by the Ministry of Science, ICT and Future Planning (NRF-2018R1D1A1B07040293), and Research Assistance Program (2019) in the Incheon National University.

Author contributions

JTP and SCP conceived of and designed the experiments. JWL, MUK and JTP performed the experiments. JWL, MUK, HEC and JTP analyzed the data. JWL, MUK, JTP and SCP wrote and edited the paper.

Declaration of competing interest

The authors declare no competing financial interests.

References

Ascierto, P.A., Kirkwood, J.M., Grob, J.-J., Simeone, E., Grimaldi, A.M., Maio, M., Palmieri, G., Testori, A., Marincola, F.M., Mozzillo, N., 2012. The role of BRAF V600 mutation in melanoma. J. Transl. Med. 10.

Barzilai, N., Huffman, D.M., Muzumdar, R.H., Bartke, A., 2012. The critical role of metabolic pathways in aging. Diabetes 61, 1315–1322.

Bassaneze, V., Miyakawa, A.A., Krieger, J.E., 2013. Chemiluminescent detection of senescence-associated beta galactosidase. Methods Mol. Biol. 965, 157–163.

Bolden, J.E., Lowe, S.W., 2015. 15 - cellular senescence. In: Mendelsohn, J., Gray, J.W., Howley, P.M., Israel, M.A., Thompson, C.B. (Eds.), The Molecular Basis of Cancer (Fourth Edition). Content Repository Only!, Philadelphia.

Brand, M.D., Nicholls, D.G., 2011. Assessing mitochondrial dysfunction in cells. Biochem. J. 435, 297–312.

Brunk, U.T., Terman, A., 2002. Lipofuscin: mechanisms of age-related accumulation and influence on cell function. Free Radic. Biol. Med. 33, 611–619.

Cheng, L., Lopez-Beltran, A., Massari, F., MacLennan, G.T., Montironi, R., 2018. Molecular testing for BRAF mutations to inform melanoma treatment decisions: a move toward precision medicine. Mod. Pathol. 31, 24–38.

Cho, S., Hwang, E.S., 2011. Chapter 7 - fluorescence-based detection and quantification of features of cellular senescence. In: Darzynkiewicz, Z., Holden, E., Orfao, A., Telford, W., Wlodkowic, D. (Eds.), Methods in Cell Biology. Academic Press.

Dimri, G.P., Lee, X., Basile, G., Acosta, M., Scott, G., Roskelley, C., Medrano, E.E., Linskens, M., Rubelj, I., Pereira-Smith, O., 1995. A biomarker that identifies senescent human cells in culture and in aging skin in vivo. Proc. Natl. Acad. Sci. U. S. A. 92, 9363–9367.

Din, S., Konstandin, M.H., Johnson, B., Emathinger, J., Völkers, M., Toko, H., Collins, B., Ormachea, L., Samse, K., Kubli, D.A., De La Torre, A., Kraft, A.S., Gustafsson, A.B., Kelly, D.P., Sussman, M.A., 2014. Metabolic dysfunction consistent with premature aging results from deletion of Pim kinases. Circ. Res. 115, 376–387.

Guo, S., Liang, Y., Murphy, S.F., Huang, A., Shen, H., Kelly, D.F., Sobrado, P., Sheng, Z., 2015. A rapid and high content assay that measures cyto-ID-stained autophagic compartments and estimates autophagy flux with potential clinical applications. Autophagy 11, 560–572.

Haq, R., Fisher, D.E., Widlund, H.R., 2014. Molecular pathways: BRAF induces bioenergetic adaptation by attenuating oxidative phosphorylation. Clin. Cancer Res. 20, 2257–2263.

Houtkooper, R.H., Argmann, C., Houten, S.M., Cantó, C., Jeninga, E.H., Andreux, P.A., Thomas, C., Doenlen, R., Schoonjans, K., Auwerx, J., 2011. The metabolic footprint of aging in mice. Sci. Rep. 1.

Hussain, M.R.M., Baig, M., Mohamoud, H.S.A., Ulhaq, Z., Hoessli, D.C., Khogeer, G.S., Al-Sayed, R.R., Al-Aama, J.Y., 2015. BRAF gene: from human cancers to developmental syndromes. Saudi J. Biol. Sci. 22, 359–373.

Hwang, E., Yoon, G., Kang, H., 2009. A comparative analysis of the cell biology of senescence and aging. Cell. Mol. Life Sci. 66, 2503–2524.

James, E.L., Michalek, R.D., Pitiyage, G.N., de Castro, A.M., Vignola, K.S., Jones, J., Mohney, R.P., Karoly, E.D., Prime, S.S., Parkinson, E.K., 2015. Senescent human fibroblasts show increased glycolysis and redox homeostasis with extracellular metabolomes that overlap with those of irreparable DNA damage, aging, and disease. J. Proteome Res. 14, 1854–1871.

Jensen, T., Holten-Rossing, H., Svendsen, I.M., Jacobsen, C., Vainer, B., 2016. Quantitative analysis of myocardial tissue with digital autofluorescence microscopy. J. Pathol. Inform. 7, 15.

Jung, T., Hohn, A., Grune, T., 2010. Lipofuscin: detection and quantification by microscopic techniques. Methods Mol. Biol. 594, 173–193.

Kang, H.T., Hwang, E.S., 2009. Nicotinamide enhances mitochondria quality through autophagy activation in human cells. Aging Cell 8, 426–438.

Kang, H.T., Park, J.T., Choi, K., Choi, H.J.C., Jung, C.W., Kim, G.R., Lee, Y.S., Park, S.C., 2017a. Chemical screening identifies ROCK as a target for recovering mitochondrial function in Hutchinson-Gilford progeria syndrome. Aging Cell 16, 541–550.

Kang, H.T., Park, J.T., Choi, K., Kim, Y., Choi, H.J.C., Jung, C.W., Lee, Y.-S., Park, S.C., 2017b. Chemical screening identifies ATM as a target for alleviating senescence. Nat. Chem. Biol. 13, 616–623.

Kilbey, A., Terry, A., Cameron, E.R., Neil, J.C., 2008. Oncogene-induced senescence: an essential role for Runx. Cell cycle (Georgetown, Tex) 7, 2333–2340.

Kuk, M.U., Kim, J.W., Lee, Y.S., Cho, K.A., Park, J.T., Park, S.C., 2019. Alleviation of senescence via ATM inhibition in accelerated aging models. Mol. Cells 42, 210–217.

Lin, S.S., Manchester, J.K., Gordon, J.I., 2001. Enhanced gluconeogenesis and increased energy storage as hallmarks of aging in Saccharomyces cerevisiae. J. Biol. Chem. 276, 36000–36007.

Liu, X., Ding, J., Meng, L., 2018. Oncogene-induced senescence: a double edged sword in cancer. Acta Pharmacol. Sin. 39, 1553–1558.

Marani, E., Usunoff, K.G., Feirabend, H.K.P., 2009. Lipofuscin and lipofuscinosis. In: Squire, L.R. (Ed.), Encyclopedia of Neuroscience. Academic Press, Oxford.

Mayers, R.M., Butlin, R.J., Kilgour, E., Leighton, B., Martin, D., Myatt, J., Orme, J.P., Holloway, B.R., 2003. AZD7545, a novel inhibitor of pyruvate dehydrogenase kinase 2 (PDHK2), activates pyruvate dehydrogenase in vivo and improves blood glucose control in obese (fa/fa) Zucker rats. Biochem. Soc. Trans. 31, 1165–1167.

Moore, W.A., Davey, V.A., Weindruch, R., Walford, R., Ivy, G.O., 1995. The effect of caloric restriction on lipofuscin accumulation in mouse brain with age. Gerontology 41 (Suppl. 2), 173–185.

Ohya, Y., Umemoto, N., Tanida, I., Ohta, A., Iida, H., Anraku, Y., 1991. Calcium-sensitive cls mutants of Saccharomyces cerevisiae showing a Pet-phenotype are ascribable to defects of vacuolar membrane H(+)-ATPase activity. J. Biol. Chem. 266, 13971–13977.

Park, J.T., Kang, H.T., Park, C.H., Lee, Y.S., Cho, K.A., Park, S.C., 2018. A crucial role of ROCK for alleviation of senescence-associated phenotype. Exp. Gerontol. 106, 8–15.

Patil, C.K., Mian, I.S., Campisi, J., 2005. The thorny path linking cellular senescence to organismal aging. Mech. Ageing Dev. 126, 1040–1045.

Pérez-Lorenzo, R., Zheng, B., 2012. Targeted inhibition of BRAF kinase: opportunities and challenges for therapeutics in melanoma. Biosci. Rep. 32, 25–33.

Serrano, M., Lin, A.W., McCurrach, M.E., Beach, D., Lowe, S.W., 1997. Oncogenic ras provokes premature cell senescence associated with accumulation of p53 and p16INK4a. Cell 88, 593–602.

Shintani, T., Klionsky, D.J., 2004. Autophagy in health and disease: a double-edged sword. Science (New York, N.Y.) 306, 990–995.

Silva, L.P., Lorenzi, P.L., Purwaha, P., Yong, V., Hawke, D.H., Weinstein, J.N., 2013. Measurement of DNA concentration as a normalization strategy for metabolomic data from adherent cell lines. Anal. Chem. 85, 9536–9542.

Sithanandam, G., Kolch, W., Duh, F.M., Rapp, U.R., 1990. Complete coding sequence of a human B-raf cDNA and detection of B-raf protein kinase with isozyme specific antibodies. Oncogene 5, 1775–1780.

Tohma, H., Hepworth, A.R., Shavlakadze, T., Grounds, M.D., Arthur, P.G., 2011. Quantification of ceroid and lipofuscin in skeletal muscle. J. Histochem. Cytochem. 59, 769–779.

Zhu, J., Woods, D., McMahon, M., Bishop, J.M., 1998. Senescence of human fibroblasts induced by oncogenic Raf. Genes Dev. 12, 2997–3007.